PHOTONEUTRON CROSS SECTION OF OXYGEN AND ALUMINUM*

L. N. Bolen and W. D. Whitehead
Department of Physics, University of Virginia, Charlottesville, Virginia
(Received October 15, 1962)

The absolute (γ,n) cross sections of aluminum and oxygen have been measured using the bremsstrahlung from the 70-MeV synchrotron at the University of Virginia, a National Bureau of Standards type ionization chamber[1] to monitor the γ-ray beam, and a calibrated Ra-Be neutron source to measure the efficiency of the counting system. The cross section for oxygen is given in Fig. 1, where the points give the values of the experimentally determined cross sections, and the solid line is the sum of four Gaussian curves with maxima at 17.3, 19.3, 22.3, and 24.1 MeV used to synthesize the cross section. It was not possible to obtain agreement with the experimental points using curves of Lorentz shape. The cross section for aluminum is given in Fig. 2, where the points are the experimental values for the cross section, and the solid line is the sum of five Gaussian curves with maxima at 14.6, 16.4, 18.1, 19.8, and 21.4 MeV. The variables of each of the Gaussian curves used to fit the cross section data for aluminum and oxygen are shown in Tables I and II. The error bars on the cross sections in Figs. 1 and 2 give the value of the standard error at each energy point as calculated by a projection of the standard deviation at each yield point through the unfolding process, and the resulting errors as shown are slightly larger than can be attributed to the counting statistics alone.

The (γ,n) yield points were taken at 0.5-MeV intervals, using a Halpern type neutron detector[2] with eight BF_3 counters arranged in two sets. A minimum of 20 and 30 determinations were made for each yield point for aluminum and oxygen, respectively. For all points more than 2 MeV above threshold, the standard deviation of the yield determination for each point varied by less than 1% from the mean value; for instance, at 20 MeV for Al the standard deviation was 0.2%, and for oxygen at 25 MeV the standard deviation was 0.56%. The cross sections were extracted using the data from threshold to 30 MeV by the Leiss-Penfold technique[3] and using two interlacing 1-MeV bin widths.

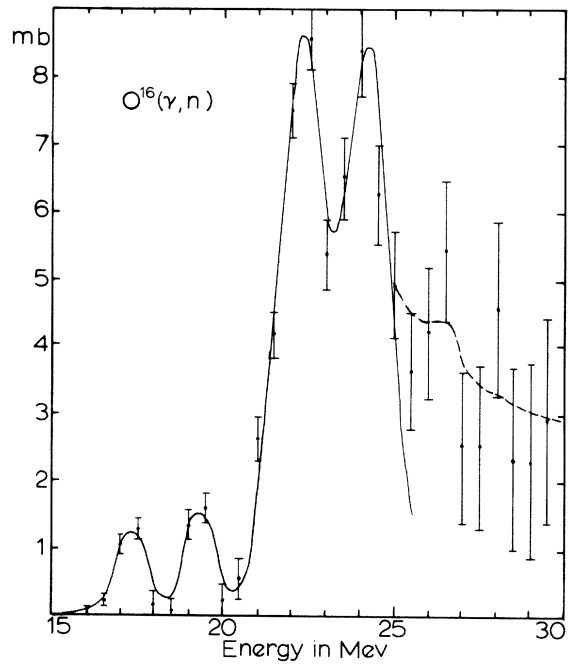

FIG. 1. $O^{16}(\gamma,n)O^{15}$ cross section. Data points are the result of this experimental determination. The solid line is the resultant of the four Gaussian curves used to synthesize the cross section.

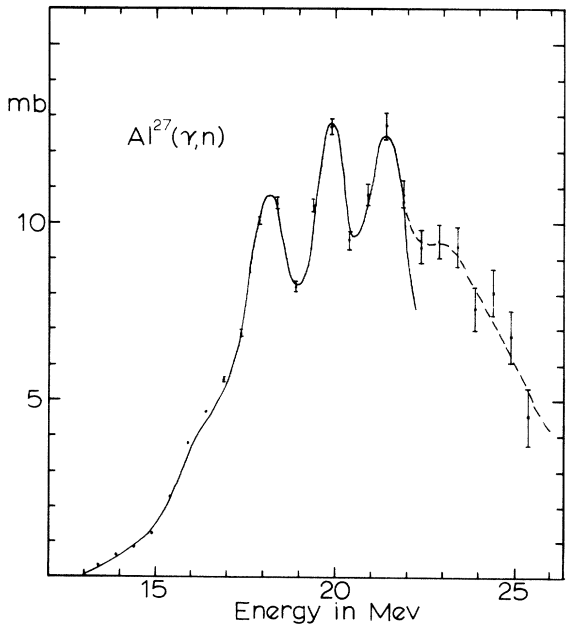

FIG. 2. $Al^{27}(\gamma,n)Al^{26}$ cross section. Data points are the result of this experimental determination. The solid line is the resultant of five Gaussian resonances used to synthesize the cross section.

Table I. The values of the parameters of the Gaussian curves used to synthesize the O^{16} cross section in Fig. 1. E_m is the energy at which the maximum cross section occurs, σ_m is the maximum cross section, and Γ is the width at half maximum of the Gaussian curve. The theoretical values of E_m, of the dipole absorption strength, and of Γ are also given.

E_m (MeV)	σ_m (mb)	Γ (MeV)	$\int\sigma(E)dE$ (MeV-mb)	E_m (theor)[a] (MeV)	% Dipole[a] strength	Γ_{theor}[b] (MeV)
17.3	1.3	1	1.5	18.1	1.0	
19.3	1.6	1	1.8	19.7	2.1	
22.3	8.4	1.7	15.2	22.6	67.9	0.64
24.1	8.3	1.7	14.9	25.4	26.0	1.12

[a]See reference 16.
[b]See reference 18.

The counting efficiency and ion chamber drift were monitored daily and varied less than 1% during the course of the runs. The oxygen target was demineralized water encased in a thin-walled glass cylinder 8 cm in length, and a similar holder was used for background determinations. The aluminum sample was a cylinder 3.8 cm in diameter and 12.7 cm in length of high-purity aluminum (99.97%). The energy scale of the synchrotron had been established by determining the (γ,n) thresholds[4] for Bi, Mn, Au, P, and C with less than 100 keV uncertainty at 15 MeV.

Since oxygen-16 has closed shells for neutrons and protons, the photon absorption cross section has been of considerable theoretical and experimental interest. The positions of the dipole states were first calculated by Elliott and Flowers,[5] and the resonances in the proton capture[6] in $N^{15}(p,\gamma)$ confirmed the existence of the two strongest transitions, with evidence of weaker transitions. Other experiments—the energy spectrum of fast neutrons,[7,8] the energy spectrum of protons,[9-12] and the (γ,n) cross section[13-15] up to 23 MeV—have confirmed the existence of the states, and in this experiment we have measured the absolute (γ,n) cross section to 30 MeV. The four strong transitions are observed, and the energies are compared with the most recent calculations[16,17] in Table I in which the integrated cross sections are also given. The neutron emission widths for the two major dipole states have been calculated[18] and are also given in Table I. The integrated cross section over the two strongest transitions is 30.1 MeV-mb, compared to 27 MeV-mb for the (γ,p) process.[12]

There have been a number of determinations[19] of the $Al^{27}(\gamma,n)$ cross section relative to copper, and only one has shown evidence for more than one resonance.[20] The total absorption cross section has been determined,[21,22] and there are resonances in the data of Dular et al.[21] at 15.8, 18.5, 20.3, and 21.8 MeV, which agree with those found here within 0.5 MeV.

Table II. The values of the parameters of the Gaussian curves used to synthesize the Al^{27} cross section in Fig. 2. E_m is the energy at which the maximum cross section occurs, σ_m is the maximum cross section, and Γ is the width at half maximum of the Gaussian curve. The experimental values of E_m determined from a total absorption experiment[a] are also given.

E_m (MeV)	σ_m (MeV)	Γ (MeV)	$\int\sigma dE$ (MeV-mb)	E_m[a] (MeV)
14.6	1	1.7	1.77	
16.4	3.6	1.7	6.37	15.8
18.1	10.6	1.7	18.8	18.5
19.8	11.2	1.2	13.9	20.3
21.4	12.5	1.7	22.1	21.8

[a]See reference 21.

*This work was supported by the U. S. Atomic Energy Commission.

[1]J. S. Pruitt and S. R. Domen, Determination of Total X-Ray Beam Energy with a Calibrated Ionization Sample, National Bureau of Standards Monograph 48 (U. S. Government Printing Office, Washington, D. C., 1962).

[2]P. A. Flournoy, R. S. Tickle, and W. D. Whitehead, Phys. Rev. 120, 1424 (1960).

[3]A. S. Penfold and J. E. Leiss, Phys. Rev. 114, 1332 (1959).

[4]K. N. Geller, J. Halpern, and E. G. Muirhead, Phys. Rev. 118, 1302 (1960).

[5]J. P. Elliott and B. H. Flowers, Proc. Roy. Soc. (London) A242, 57 (1957).

[6]S. G. Cohen, P. S. Fisher, and E. K. Warburton,

Phys. Rev. Letters 3, 433 (1959).
[7]F. W. K. Firk and K. H. Lokan, Phys. Rev. Letters 8, 321 (1962).
[8]C. Milone and A. Rubbino, Nuovo cimento 13, 1035 (1959).
[9]S. A. E. Johansson and B. Forkman, Arkiv Fysik 12, 359 (1957).
[10]P. Brix and E. K. Maschke, Z. Physik 155, 109 (1959).
[11]D. L. Livesey, Can. J. Phys. 34, 1022 (1956).
[12]W. R. Dodge and W. C. Barber, Phys. Rev. 127, 1746 (1962).
[13]J. Miller, G. Schuhl, G. Tamas, and C. Tzara, Phys. Letters 2, 76 (1962).
[14]B. M. Spicer, Australian J. Phys. 10, 326 (1957).
[15]K. N. Geller, Phys. Rev. 120, 2147 (1960).
[16]V. Gillet and N. Vinh Mau, Phys. Letters 1, 25 (1962).
[17]G. E. Brown, L. Castillejo, and J. A. Evans, Nuclear Phys. 22, 1 (1961).
[18]M. Bauer, Ph.D. thesis, University of Maryland, 1962 (unpublished).
[19]F. Ferrero, R. Malvano, S. Menardi, and O. Terracini, Nuclear Phys. 9, 32 (1958).
[20]J. E. E. Baglin, N. M. Thompson, and B. M. Spicer, Nuclear Phys. 22, 207 (1961).
[21]J. Dular, G. Kernel, M. Kregar, M. V. Mihailovic, G. Pregl, M. Rosina, and C. Zupancic, Nuclear Phys. 14, 131 (1959).
[22]B. Ziegler, Nuclear Phys. 17, 239 (1960).

FINAL-STATE INTERACTIONS IN THE $\pi^- + p \to K + \bar{K} + N$ REACTION*

Gideon Alexander,† Orin I. Dahl, Laurance Jacobs, George R. Kalbfleisch, Donald H. Miller, Alan Rittenberg, Joseph Schwartz, and Gerald A. Smith
Department of Physics and Lawrence Radiation Laboratory, University of California, Berkeley, California
(Received October 29, 1962)

In this Letter we report results of a study of the reaction $\pi^- + p \to K + \bar{K} + N$ at incident momenta less than 2.3 BeV/c. We find that the distribution in momentum transfer to the recoil nucleon is consistent with the assumption that most $K\bar{K}$ pairs are produced in peripheral $\pi^- + p$ collisions, as suggested by the data of Erwin et al.[1] However, the effective-mass distributions for the $\bar{K}N$ system indicate that an additional contribution to the $K\bar{K}N$ final state arises from production of the isotopic spin $I=0$ resonant state $Y_0^*(1520\ \text{MeV})$,[2] with the subsequent decay $Y_0^* \to \bar{K} + N$. We have also examined the $K\bar{K}$ effective-mass distributions for possible effects due to final-state interactions. Although the K^0K^- effective-mass distribution is consistent with the phase-space estimate, an enhancement is observed for the neutral $K\bar{K}$ system (K_1K_1n final states) in the region $M^2(K_1K_1) \simeq (1.02\ \text{BeV})^2$. A satisfactory fit to the data is obtained if the enhancement is attributed to strong scattering in the $I=0$, S-wave $K\bar{K}$ state. In a study of the reaction $K^- + p \to \Lambda + K + \bar{K}$ at 2.24 and 2.5 BeV/c, Bertanza et al. have observed a similar enhancement at approximately the same mass; however, only final states of the type ΛK_1K_2 were found.[3] The relation of the two results is discussed.

The data were obtained during an extensive exposure of the Lawrence Radiation Laboratory's 72-in. hydrogen bubble chamber to a secondary π^- beam at six momentum settings ranging from 1.51 to 2.25 BeV/c. A total of 225 000 pictures with 10 to 20 π^- mesons each were taken and scanned for visible production of strange particles. Of the 12 000 events measured, 158 were unambiguously identified via the kinematical constraint program PACKAGE as belonging to one of the following hypotheses:

(a) $\pi^- + p \to K^0 + K^- + p$, with $K^0 \to \pi^+ + \pi^-$;

(b) $\pi^- + p \to K^0 + \bar{K}^0 + n$, with $K^0 \to \pi^+ + \pi^-$, and $\bar{K}^0 \to \pi^+ + \pi^-$.

The number of observed events together with the approximate path length examined is summarized in Table I.

The Dalitz plot for the reaction $\pi^- + p \to K^0 + K^- + p$, together with its projections on the $M^2(K^0K^-)$ and $M^2(K^-p)$ axes, is shown in Fig. 1. Since the effects of two-body interactions may be obscured in events occurring too close to the kinematic threshold, all events for which the laboratory momentum of the incident pion p_π is less than 1.95 BeV/c have been plotted separately and are not used in the analysis of effective-mass distributions. The phase-space curves represent weighted averages for the data appearing in the plots. A strong enhancement appears in the $M^2(K^-p)$ distribution at $M^2 \simeq (1520\ \text{MeV})^2$, with estimated full width $\Gamma \simeq 25$ MeV. Since the resonant state, Y_0^*(152 MeV, is readily produced in the π^- momentum